33RD INTERNATIONAL COSMIC RAY CONFERENCE, RIO DE JANEIRO 2013
THE ASTROPARTICLE PHYSICS CONFERENCE

ICRC 2013

Ground Level Enhancement of May 17, 2012 Observed at South Pole

THE ICECUBE COLLABORATION[1]

[1]*See special section in these proceedings*

Abstract: Amundsen Scott station, located at the geographic South Pole, is arguably the most sensitive surface location on Earth for the detection of solar energetic particles because of the combination of low geomagnetic cutoff and high altitude. Three complementary instruments are now in operation there. IceTop is an array of 162 ice Cherenkov detectors each comprising approximately 2000 kg of clear ice. Each detector is viewed by photomultipliers feeding rate scalers set to different threshold levels, typically counting 1 kilohertz and above. The array of thresholds in principle allows IceTop to determine the energy spectrum of the solar energetic particles. The South Pole neutron monitor, with a long operating history at this location, is a standard 3NM64. Additionally there is an array of bare neutron detectors (without lead shielding) referred to as the Polar Bares. The monitor and bares respond to successively lower energy particles than the Cherenkov detectors, extending the spectral response. In this work we examine the Ground Level Enhancement (GLE) of May 17, 2012, related to an M5.1 solar flare, which was the first GLE in this solar cycle and the first one since December 2006. We estimate the energy spectrum of the solar particles and interpret the result in the context of observations from the global neutron monitor network. **Corresponding authors:** Takao Kuwabara[2], Paul Evenson[2]

[2] *University of Delaware, 217 Sharp lab, Newark DE 19711, USA*

Keywords: IceCube, IceTop, Neutron Monitor, Ground Level Enhancement, Solar Flare

1 Introduction

The Amundsen Scott station is located at the geographic South Pole. With its unique position of high altitude (2835m) and nearly zero geomagnetic cut-off, cosmic ray detectors located there can resolve solar and galactic cosmic ray disturbances with unprecedented detail. Three complementary instruments are now in operation there. One is a standard 3NM64 neutron monitor [1] and another is an array of 12 bare (without lead) neutron detectors referred to as the Polar Bares.

The third is IceTop, the surface component of the IceCube Neutrino Observatory, which is an air shower array consisting of 162 ice Cherenkov "tank" detectors, each 90 cm deep and each with a surface area of 2.7 m^2. In each tank the Cherenkov light is measured by two Digital Optical Modules (DOM), one operated at high gain and the other at low gain to provide sufficient dynamic range to cover both large and small air showers. For the analysis of solar events, we use counting rates from two discriminators in each high gain DOM. For historical reasons the discriminators are termed SPE (Single Photo Electron) and MPE (Multi Photo Electron). The SPE discriminators are in fact set to thresholds ranging from below one photoelectron to over 20 photoelectrons. All of the MPE discriminators are set to a threshold of approximately 20 photoelectrons as needed for air shower detection. Counting rates of the SPE discriminators range from 1 to 15 kHz. Those SPE and MPE discriminator rates are affected by the different amount of snow that has accumulated on each tank [2].

In a ground based cosmic ray detector the fine details of the primary spectrum at the top of the atmosphere for solar physics work are lost but, particularly at South Pole, a surprising amount of information remains. Yield functions, with units area-solid-angle, describe the relation between particle flux at the top of the atmosphere and a particular counting rate. They depend on particle arrival direction, rigidity, mass of the primary nucleus and detector characteristics. At high latitudes such as South Pole, defocusing in the geomagnetic field produces a nearly isotropic flux at the top of the atmosphere even if the flux outside the magnetosphere is highly anisotropic. At low energy (when the probability of a particle or its progeny to reach the surface is small), the yield function is smaller than the physical area-solid-angle of the detector, but at high energy (when a shower can give rise to a signal even if the extrapolated trajectory of the primary passes outside the detector) it can be larger. The yield function of the Polar Bares peaks at lower energy than that of the 3NM64. IceTop yield functions peak at still higher energies, with each discriminator threshold producing a different yield function.

In this paper we examine the Ground Level Enhancement (GLE) of May 17, 2012, related to an M5.1 solar flare, which was the first GLE in this solar cycle and the first one since December 2006. By using calculated and measured yield functions for the various detectors we are able to deconvolute the different discriminator counting rates to produce an estimate of the energy spectrum of the solar particles and interpret the result in the context of observations from the global neutron monitor network.

2 GLE Observation from the Neutron Monitor Network

An overview of the GLE as seen in the neutron monitor network is shown in Figure 1. Onset was around 1:50 UT at Apatity and Oulu, both of which had viewing directions close to the inferred sunward direction of the interplanetary magnetic field (IMF). Mawson, which actually views closer

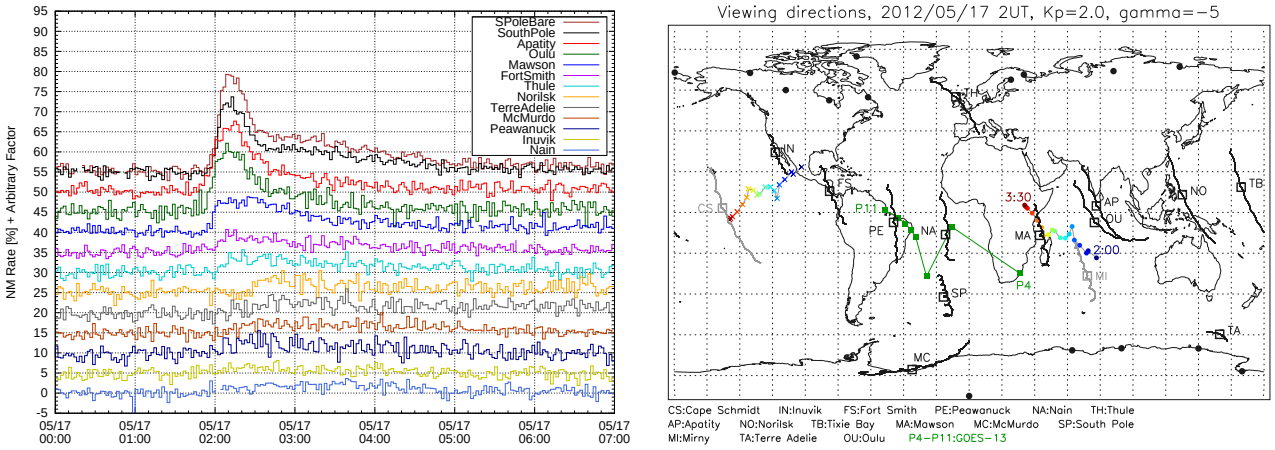

Figure 1: Percent increases, relative to the count rate averaged from 01:00 to 01:30 UT of 11 high latitude neutron monitors with arbitrary values added to separate the traces [3, 4] (left) and viewing directions for an assumed P^{-5} particle spectrum calculated for 2:00 UT (right). Solid circles show station locations, squares show asymptotic viewing directions for a median energy particle, and lines show the range of viewing directions for the central 80% of the detector energy response. Viewing directions for the GOES-13 P4-P11 channels are also shown. The IMF direction at Earth [5] from 2:00 to 3:30 UT is shown as a series of colored marks, solid circles for the sunward direction and x marks for the anti-sunward.

to the inferred field direction also saw a fast rise however the peak was not clearly observed and intensity was about half of others (8%). It is not unusual to see an offset of the peak fluxes from the inferred field direction. Other stations with less favorable viewing directions saw smaller enhancements as is typical. The South Pole NM64 and Polar Bare increases started a few minutes after Apatity and Oulu and showed a clear pulse like enhancement ($\geq$15%) with a peak just after 2:00 UT even though their viewing direction is more comparable to that of Peawanuck and Nain, which saw relatively small increases. All of those stations see broader enhancements ($\geq$ 5%) behind the pulse. Other stations see only broad enhancements but with small ($\leq$ 5%) amplitudes.

3 GLE Observation at South Pole

Figure 2 compares the GLE observed at South Pole with data from the GOES-13 spacecraft [6] which had a similar asymptotic direction. IceTop rates are average counting rate of several discriminators. SPE1 and SPE2 are the average of the lower 62 and higher 100 SPE discriminator thresholds respectively, while MPE is the average of all 162 MPE discriminators. We can see that lower threshold discriminators have larger percentage increases. The Bare count rates also have a larger percentage increase than the NM64 rates because they respond more to lower energy particles and the solar spectrum is softer than the galactic cosmic ray spectrum. We can see that IceTop and neutron monitors both saw the clear pulse and subsequent broad enhancement. In this preliminary analysis we use the counting rates of the multiple discriminator thresholds in IceTop and the different neutron detectors to derive the energy spectrum of the solar particles during the initial pulse of the event.

3.1 NM and Polar Bare Analysis

If we assume that the galactic cosmic ray flux is constant during the baseline interval and throughout the enhancement, the neutron monitor counting rate increase at the location of geomagnetic cut-off rigidity P_c is expressed as

$$\Delta N(P_c) = \int_{P_c}^{\infty} S(P) \cdot J_{sep}(P) dP \qquad (1)$$

where $S(P)$ is the NM yield function and $J_{sep}(P)$ is the primary solar energetic particle (SEP) spectrum. By assuming a simple power law SEP spectrum as $J_{sep}(P) = J_0 P^{-\gamma}$, the ratio of rate increases of Bare to NM64 can be expressed as a function of γ

$$\frac{\Delta N_{Bare}}{\Delta N_{NM64}} = \frac{\int_{P_c}^{\infty} S_{Bare} \cdot P^{-\gamma} dP}{\int_{P_c}^{\infty} S_{NM64} \cdot P^{-\gamma} dP} \qquad (2)$$

Response functions for Bare S_{Bare} and NM64 S_{NM64} are determined in [7] from Dorman functions $N(P) = N_0(1 - exp(-\alpha P^{-k}))$ which have parameters N_0=157.68, α=7.846, and k=0.940 for Bare, and N_0=151.67, α=8.415, and k=0.894 for NM64.

We then follow [8] to derive the spectrum of the solar particles. Spectral parameters shown in the bottom two panels of Figure 2 are determined every 10 min from 2:00 to 4:30 (points), along with a 15 min average from 02:05 to 02:20 UT for the pulse and a 60 min average from 02:35 to 03:35 UT for the broad enhancement (bars). These averages and time intervals are used in the subsequent comparison with IceTop. We derive a somewhat harder spectrum for the pulse ($J_{sep}(P) = 1.14 \cdot P^{-4.3}$(cm^2 s sr GV)$^{-1}$, P in GV) than for the broad enhancement ($J_{sep}(P) = 0.673 \cdot P^{-4.9}$(cm^2 s sr GV)$^{-1}$, P in GV).

3.2 Spectrum from IceTop

Figure 3 shows the increase in counting rate of individual IceTop discriminators averaged over 15 min from 02:05 to 02:20 UT. These increases are plotted as a function of the base count rates defined as an average count rate from 01:00 to 01:30 UT. Discriminators with higher base count rates (lower threshold settings) have larger increases. In

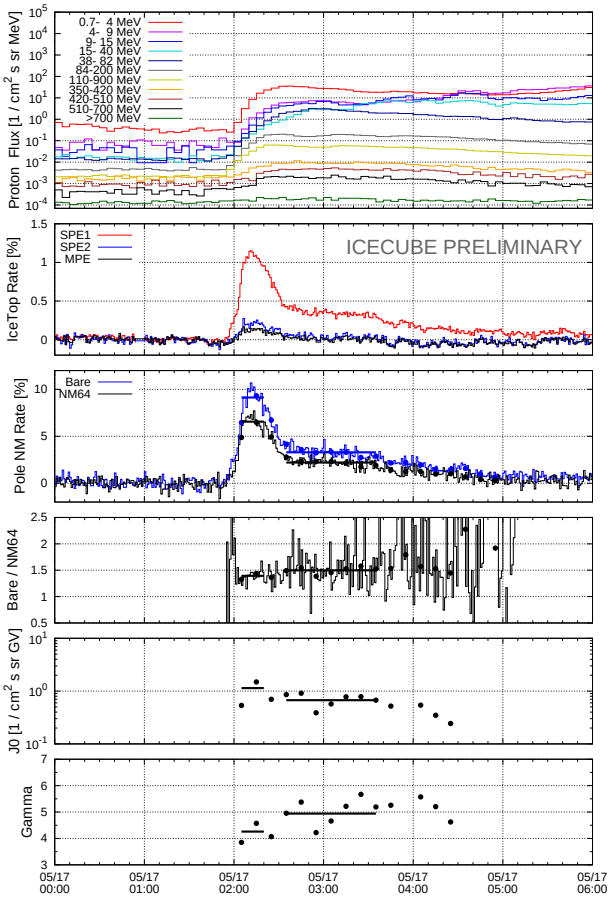

Figure 2: GLE observation at South Pole and GOES. From top panel, GOES-13 proton channel, IceTop rates, South-Pole neutron monitor rates, ratio of Bare/NM64 monitor, estimated parameters of primary spectrum from "Polar Bare" analysis as amplitude J0 and exponent γ of a power law in momentum.

order to derive a spectrum from the counting rates we must determine a separate yield function for each discriminator. The yield functions must minimally take into account the discriminator setting, characteristics of the tank, barometric pressure and snow cover, all on an individual basis.

Determining a complete set of yield functions is a work in progress. We are presently engaged in adapting the extensive simulation apparatus developed to analyze air showers with IceTop [10]. Significant modification is required because the minimum signal accepted in the air shower analysis corresponds to the MPE threshold, approximately 20 photoelectrons, whereas most of the information on solar events comes from signals with amplitudes below this. Simulation of signals above 20 photoelectrons is well developed on an integrated charge basis, whereas at lower levels the shape of the waveform becomes more irregular and the treatment must be on a voltage amplitude basis. In Figure 3 note the rather regular behavior of the increases for base rates below 4 kHz and the markedly different behavior to the right of this. The threshold producing a base rate of 4 kHz is predicted by the integrated charge calibration to correspond to 3 photoelectrons which defined as the half of the maximum value of the charge distribution [10]. Observationally however, 4 kHz is clearly the true single photoelectron threshold. Lower thresholds produce increasing base rates as they go deeper into the electronic noise but the enhancements during the event do not get larger as one photoelectron is the minimum signal that can be generated physically.

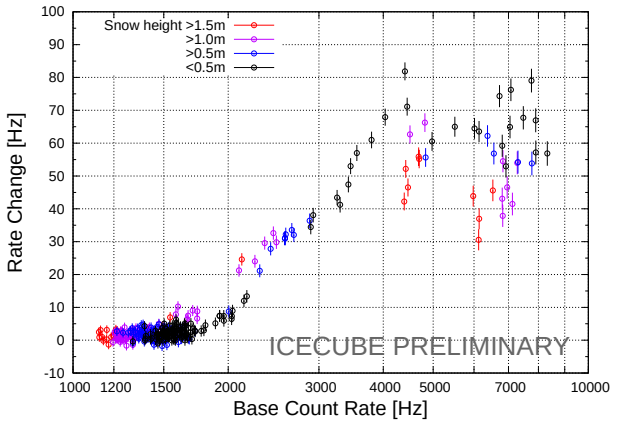

Figure 3: Increase of individual IceTop discriminator counting rates during the pulse above the base count rates (defined as the average count from 01:00 to 01:30 UT). Different colors correspond to different snow overburden.

Until the more tailored calculations of yield functions are available we must be content to make phenomenological corrections to the data. One such correction is already implicit in Figure 3 where we have corrected all of the data for barometric pressure using multiplicative factors derived for the base rates. We can also easily derive a phenomenological correction of the snow effect to the base counting rate, this time an additive correction. When applied, as in Figure 4, this results in a much more aesthetic ordering of the data. However clear trends remain in the increases related to snow depth, as one might expect. The dashed line in Figure 4 is a calculation of the counting rate enhancements expected in IceTop based on the particle spectrum derived from the neutron monitor data.

At this point we return to the technique employed in our analysis of the 2006 December 13 event [11] where we used generic yield functions (in the sense that they were calculated for nominal tank properties, no snow overburden, and a single barometric pressure) for various discriminator settings from FLUKA simulations [12]. We derive the yield function S_i for each discriminator i from its snow corrected base counr rate N_i^{base} and an assumed galactic cosmic ray spectrum J_{gcr} as

$$N_i^{base} = \int S_i(P) J_{gcr}(P) dP. \qquad (3)$$

We can then determine the simple power law SEP spectrum J_{sep} by using a least squares fitting technique to minimize,

$$\chi^2 = \sum_i \{ \frac{1}{\sigma^2_{\Delta N_i}} [\Delta N_i - \int S_i(P) J_{sep}(P) dP]^2 \}, \qquad (4)$$

where ΔN_i is the rate changes in i-th discriminator. From the FLUKA simulation 3.6 kHz is the rate at the single photoelectron setting, so we apply the fitting to the discriminators for which the base count rate is lower than that. The solid line in Figure 4 shows the calculated enhancements

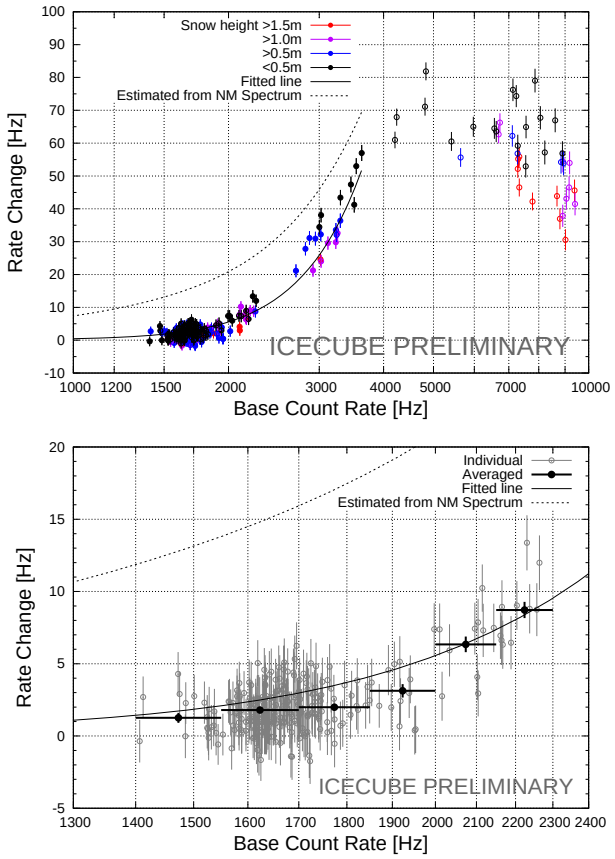

Figure 4: Increase of individual IceTop discriminator counting rates during the pulse above snow corrected base count rates. Solid line is the best fit to a power law (in rigidity) spectrum, dashed line is enhancement estimated from the neutron monitor spectrum. Bottom panel is an enlargement of the high threshold region. Gray circles are individual rate and black solid points are averaged value of them.

based on the derived spectrum ($J_{sep}(P) = 16.7 \cdot P^{-10}$(cm^2 s sr GV)$^{-1}$, P in GV).

4 Summary

Figure 5 summarizes different determinations of the spectrum. The solid line is the spectrum from the Monitor / Polar Bare analysis with the heavier line denoting the range (0.7−7.5 GeV) that contains central 80% of the energy response of the monitors to the solar particles. Points are the measurement of proton flux from the GOES 13 spacecraft. The basic consistency of the two measurements is similar to that obtained in an analysis of multiple events by [13]. The dashed line, from IceTop analysis, is not consistent with the neutron monitor analysis in that it lies below the solid line over most of the response range of the monitors. This confirms the visual impression from Figure 4, in which the prediction of the IceTop response from the neutron monitor spectrum lies significantly above all of the actual data points. However the agreement is much better at lower threshold (higher count rate) where the discrepancy is perhaps 15% whereas at the higher thresholds the discrepancy is a factor of ten or more. Our present interpretation is that the dramatically steeper spectrum observed by IceTop must be taken

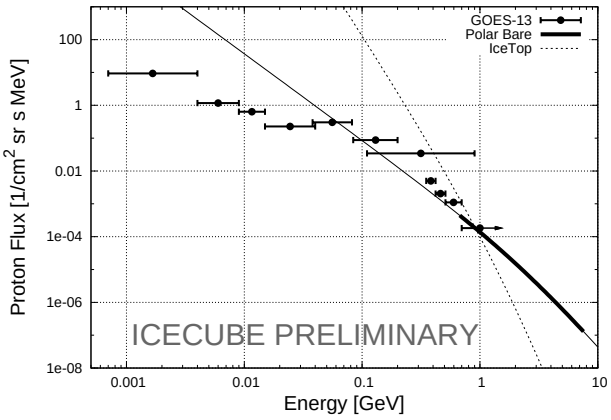

Figure 5: Proton spectrum determined from Neutron Monitor Polar Bare analysis (line) and IceTop analysis (dashed line). The points are the proton fluxes from GOES-13 spacecraft data.

seriously. The most probable explanation is that the true spectrum exhibits a major steepening but at a significantly higher energy than might be indicated by the lines in Figure 5 and therefore cannot be adequately represented by a power law in rigidity in either detector. Further progress from this point must await improved calculations of the IceTop yield functions and calculations of the neutron monitor and bare yield functions within the same framework.

Acknowledgment: We acknowledge the NMDB database (www.nmdb.eu), founded under the European Union's FP7 programme (contract no. 213007) for providing neutron monitor data of Terre Adelie - French Polar Institute (IPEV), France, Oulu - University of Oulu, Finland, Apatity - Polar Geophysical Institute, Russia, and Norilsk - Institute of Solar-Terrestrial Physics (ISZF), Russia. We also thank Marc Duldig and IPS Radio and Space Services, Bureau of Meteorology, Australia for providing Mawson neutron monitor data. We thank John Bieber, John Clem, David Ruffolo, Roger Pyle and Alejandro Saiz for scientific discussions and for help with preparing the data from the University of Delaware neutron monitors. In addition to US National Science Foundation support for IceCube, the South Pole neutron detectors operated under award ANT-0838839 and the McMurdo neutron monitors under ANT-0739620 .

References

[1] P. H. Stoker, L. I. Dorman, and J. M. Clem, Space Science Reviews 93 (2000) 361-380.
[2] IceCube Collaboration, paper 1106, these Proceedings.
[3] http://www.nmdb.eu/
[4] Duldig, M. (private communication, 2013)
[5] http://omniweb.gsfc.nasa.gov
[6] http://www.swpc.noaa.gov/Data/goes.html
[7] P. H. Stoker, Proc. 19th ICRC, La Jolla, 4 (1985) 114-117.
[8] J. W. Bieber and P. Evenson, Proc. 22nd ICRC, Dublin, 3 (1991) 129-132.
[9] J. W. Bieber and P. Evenson, Proc. 24th ICRC, Roma, 4 (1995) 1316-1319.
[10] R. Abbasi et al., IceCube Collaboration, NIM-A 700 (2013) 188-220.
[11] R. Abbasi et al., IceCube Collaboration, The Astrophysical Journal Letters 689 (2008) L65-L68.
[12] J. M. Clem, P. Niessen, and S. Stoyanov, Proc. 30th ICRC, Merida, 1 (2007) 237-240.
[13] S. Oh, J. W. Bieber, J. M. Clem, P. Evenson, R. Pyle, Y. Yi, and Y.-K. Kim, Space Weather (2012), doi:10.1029/2012SW000795.